

A New Insight into Using Chlorine Leaving Group and Nucleophile Carbon Kinetic Isotope Effects To Determine Substituent Effects on the Structure of S_N2 Transition States

Kenneth C. Westaway,^{*,†} Yao-ren Fang,[†] Susanna MacMillar,[‡] Olle Matsson,^{*,‡}
Raymond A. Poirier,^{*,§} and Shahidul M. Islam[§]

Department of Chemistry and Biochemistry, Laurentian University, Sudbury, Ontario P3E 2C6, Canada,
Department of Biochemistry and Organic Chemistry, Uppsala University, P.O. Box 576, SE-751 23 Uppsala,
Sweden, and Department of Chemistry, Memorial University, St. John's, Newfoundland and Labrador A1B
3X7, Canada

Received: April 17, 2007

Chlorine leaving group k^{35}/k^{37} , nucleophile carbon k^{11}/k^{14} , and secondary α -deuterium $[(k_H/k_D)_\alpha]$ kinetic isotope effects (KIEs) have been measured for the S_N2 reactions between *para*-substituted benzyl chlorides and tetrabutylammonium cyanide in tetrahydrofuran at 20 °C to determine whether these isotope effects can be used to determine the substituent effect on the structure of the transition state. The secondary α -deuterium KIEs indicate that the transition states for these reactions are unsymmetric. The theoretical calculations at the B3LYP/aug-cc-pVDZ level of theory support this conclusion; i.e., they suggest that the transition states for these reactions are unsymmetric with a long NC–C_α and reasonably short C_α–Cl bonds. The chlorine isotope effects suggest that these KIEs can be used to determine the substituent effects on transition state structure with the KIE decreasing when a more electron-withdrawing *para*-substituent is present. This conclusion is supported by theoretical calculations. The nucleophile carbon k^{11}/k^{14} KIEs for these reactions, however, do not change significantly with substituent and, therefore, do not appear to be useful for determining how the NC–C_α transition-state bond changes with substituent. The theoretical calculations indicate that the NC–C_α bond also shortens as a more electron-withdrawing substituent is placed on the benzene ring of the substrate but that the changes in the NC–C_α transition-state bond with substituent are very small and may not be measurable. The results also show that using leaving group and nucleophile carbon KIEs to determine the substituent effect on transition-state structure is more complicated than previously thought. The implication of using both chlorine leaving group and nucleophile carbon KIEs to determine the substituent effect on transition-state structure is discussed.

Introduction

The effect of substituents on the structure of the S_N2 transition state has been of major interest for several decades.^{1–12} The major experimental tool used to determine the substituent effect on transition-state structure has been a kinetic isotope effect (KIE). Although many different types of KIEs have been used to probe the transition states of S_N2 reactions,^{4,6–9,13–17} most of the studies have used leaving group KIEs to determine the relative lengths of C_α–LG transition-state bonds.^{1,4,9,15,18} Until recently, the interpretation of these KIEs was thought to be straightforward; i.e., it was believed that a larger leaving group KIE was indicative of greater C_α–LG bond rupture in the transition state. However, a recent theoretical investigation of chlorine leaving group KIEs¹⁹ indicated that the interpretation of these KIEs was not as straightforward as had been previously thought. In fact, this study showed that all of the chlorine leaving group KIEs for 26 S_N2 reactions with methyl chloride fell in a very narrow range of values and that there was no relationship between the magnitude of the KIE and the C_α–Cl bond length in the transition state! The total KIE (k^{35}/k^{37}) is the product of

the tunneling KIE (KIE_T), the imaginary frequency ratio or temperature-independent factor (TIF), and the temperature-dependent factor (TDF) that represents the isotope effect on the vibrational contribution to the KIE,^{20,21} eq 1

$$\frac{k^{35}}{k^{37}} = \underbrace{\left(\frac{k^{35}}{k^{37}}\right)_{\text{Tunnel}}}_{\text{KIE}_T} \times \underbrace{\left(\frac{\nu^{*35}}{\nu^{*37}}\right)}_{\text{TIF}} \times \underbrace{\prod_i \frac{\mu_{i37}^R \sinh(\mu_{i35}^R/2)}{\mu_{i35}^R \sinh(\mu_{i37}^R/2)} \times \prod_i \frac{\mu_{i37}^* \sinh(\mu_{i35}^*/2)}{\mu_{i35}^* \sinh(\mu_{i37}^*/2)}}_{\text{TDF}} \quad (1)$$

where R represents the isotopically substituted reactant, ‡ indicates the transition state, $\mu_i = h\nu_i/k_B T$, and the ν_i 's are the vibrational frequencies. The relationship between the magnitude of the KIE and the C_α–Cl bond length in the transition state failed because the product of KIE_T and TIF accounted for a significant portion of the total KIE and was not related to transition-state structure in any discernible way. This meant that one could not use the magnitude of the total KIE to estimate the C_α–Cl transition-state bond length even though the TDF term of the KIE was related to the length of the C_α–Cl bond in the transition state.¹⁹ A subsequent study by Matsson, Paneth, Westaway and co-workers²² has demonstrated that one can still use a leaving group chlorine KIE to determine the length of the C_α–Cl bond in a reaction where the solvent has been varied, i.e., to determine the solvent effect on the length of the C_α–Cl bond in an S_N2 transition state. The next question was whether one could use chlorine leaving group KIEs to determine the

* Authors to whom correspondence should be addressed. E-mail: kwestaway@laurentian.ca; olle.matsson@biorg.uu.se; rpoirier@mun.ca.

† Laurentian University.

‡ Uppsala University.

§ Memorial University.

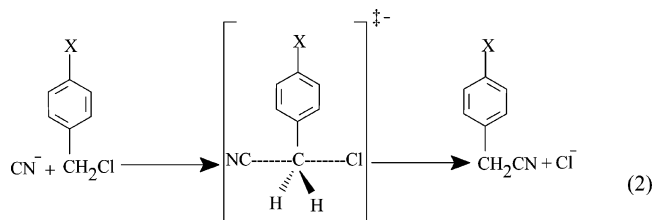
substituent effects on transition-state structure in a series of S_N2 reactions of *para*-substituted benzyl chlorides where both the KIE_T and the TIF were expected to be almost identical for each reaction in the series. An additional question was whether the nucleophile carbon KIE could be used to determine the relative length of the NC–C_α transition-state bond when the nucleophile in these reactions is cyanide ion.

Computational Method

The calculations were done at the RHF/6-31+G(d), the B3LYP/6-31+G(d), and the B3LYP/aug-cc-pVDZ levels of theory. The last method was chosen because it gave the closest KIEs to the experimental values in a thorough examination of the available methods for calculating transition-state structure and the KIEs in the ethyl chloride–cyanide ion S_N2 reaction.²³ Unscaled frequencies and no solvent were used for the calculations. All calculations were performed with Gaussian 03 using default convergence criteria.²⁴ Each transition structure had one imaginary frequency that corresponds to the transfer of the α carbon from the chlorine of the leaving group to the carbon of the cyanide ion nucleophile. The effect of tunneling on the calculations was done using the Wigner approximation.²⁵ All of the KIEs were calculated with the program ISOEFF98.²⁶

Results and Discussion

The substituent effect on the structure of the S_N2 transition state has been determined by measuring the secondary α-deuterium (*k_H/k_D*)_α, the chlorine leaving group (*k³⁵/k³⁷*), and the nucleophile carbon *k¹¹/k¹⁴* KIEs for the reactions between cyanide ion and *para*-substituted benzyl chlorides, eq 2, in tetrahydrofuran (THF) at 20 °C where X = CH₃, H, F, Cl, and NO₂.



The solvent for this study was chosen because of its very low dielectric constant of 7.3.²⁷ A recent study²² showed that a significant change in solvent does not change the structure of a type I (where the nucleophilic atoms in the transition state have the same charge) S_N2 transition state significantly, so the lack of solvent in the theoretical calculations used to determine the transition-state structures and the KIEs at several levels of theory, was not expected to have a significant effect on the results. In any case, the lowest dielectric solvent possible experimentally was used so any effect caused by the lack of solvent in the calculations would be minimized.

Secondary α-Deuterium KIEs: The secondary α-deuterium [(*k_H/k_D*)_α] KIEs were measured for only the *para*-hydrogen- and *para*-chlorobenzyl chlorides to determine the symmetry of the S_N2 transition states. Westaway et al.²⁸ found that the change in the magnitude of the (*k_H/k_D*)_α with substituent was small (≤1%) for S_N2 reactions with unsymmetric transition states and much larger (3–12%) for S_N2 reactions with symmetric (central) transition states. The (*k_H/k_D*)_α's were measured at 0 °C rather than the 20 °C that was used for the other KIEs to slow the reactions enough so that the rate constants and KIEs could be determined. This temperature difference does not affect the conclusion about the symmetry of the transition states for these

TABLE 1: Experimental Secondary α-Deuterium KIE for the S_N2 Reactions between Cyanide Ion and Benzyl- and *para*-Chlorobenzyl Chloride at 0 °C in THF

<i>para</i> -substituent	<i>k_H</i> × 10 ³ ^a (M ⁻¹ s ⁻¹)	<i>k_D</i> × 10 ³ ^a (M ⁻¹ s ⁻¹)	(<i>k_H/k_D</i>) _{α-D2}
H	2.399 ± 0.002 ^b	2.385 ± 0.001 ^b	1.006 ± 0.001 ^c
Cl	9.713 ± 0.002	9.597 ± 0.001	1.012 ± 0.001

^a The rate constant quoted is the average of the rate constants found in at least three different experiments. ^b Standard deviation. ^c The error in the KIE is 1/*k_D*[(Δ*k_H*)² + (*k_H/k_D*)² × (Δ*k_D*)²]^{1/2}, where Δ*k_H* and Δ*k_D* are the standard deviations for the average rate constants for the reactions of the undeuterated and deuterated substrates, respectively.⁵

reactions because these KIEs only decrease by approximately 0.008 when the temperature decreases by 20 °C,^{11,29,30} and more importantly, it is the difference in the KIEs for the reactions with different substituents, not the absolute magnitude of the KIEs, that is important in assessing the symmetry of S_N2 transition states. The change in the experimental (*k_H/k_D*)_α's with substituent, Table 1, is very small, i.e., approximately 0.6% for these reactions, indicating that the transition states are unsymmetric, i.e., either reactant-like or product-like. The calculations, Table 2, confirm that these reactions proceed via unsymmetric transition states. Although the calculated KIEs are slightly (about 1–2%) smaller than the experimental values, the change in the KIE with substituent is very small; e.g., the KIE at the B3LYP/aug-cc-pVDZ level of theory, the method that best reproduces the experimental KIEs,²³ only changes by 1.2% when the *para*-substituent is changed from methyl to nitro. Finally, it is important to note that the calculated transition states for this system of reactions are all reactant-like with long NC–C_α and relatively short C_α–Cl bonds; i.e., the percent extension of the NC–C_α and C_α–Cl bonds on going to the transition state at the B3LYP/aug-cc pVDZ level of theory (Table 5), eq 3, is 61 ± 1% and 22 ± 1%, respectively

% extension on going to the transition state =

$$\frac{\left[\frac{\text{bond length in the transition state} - \text{bond length in the reactant (product)}}{\text{bond length in the reactant (product)}} \right] \times 100}{\text{bond length in the reactant (product)}} \quad (3)$$

It is also important to note that the calculated KIEs indicate that the (*k_H/k_D*)_α decreases when a more electron-withdrawing substituent is on the benzene ring of the substrate. This substituent effect on the KIE has been found in almost every investigation of the (*k_H/k_D*)_α's for the reactions of *para*-substituted benzyl compounds.^{28,31} It is also important to note that the substituent effect on these calculated KIEs was checked by plotting the calculated KIEs in Table 2 against the Hammett σ value for each substituent.³² The correlation coefficient for each plot was very high, ranging from 0.954 to 0.980. It is interesting that the worst fit with the Hammett σ values is found with the calculations using the largest basis set and that the best fit is with the RHF/6-31+G(d) calculations. However, the correlation coefficients in all the Hammett σ plots are very high, giving one great confidence that the trends predicted by the calculations are correct.

Chlorine Leaving Group KIEs: The chlorine leaving group (*k³⁵/k³⁷*) KIEs were measured for the S_N2 reactions between cyanide ion and four *para*-substituted benzyl chlorides in THF at 20 °C, Table 3. The values from the original set of experiments measuring these KIEs are in column 2 of Table 3. The surprising observation is that the KIEs do not follow a single

TABLE 2: Secondary α -Deuterium (k_H/k_D) $_{\alpha}$ KIEs for the S_N2 Reactions between Cyanide Ion and Five *Para*-Substituted Benzyl Chlorides at 25 °C Using Three Different Levels of Theory

<i>para</i> -substituent	$(k_H/k_D)_{\alpha}$		
	RHF/6-31+G(d)	B3LYP/6-31+G(d)	B3LYP/aug-cc-pVDZ
CH ₃	0.9677	0.9837	0.9851
H	0.9606	0.9812	0.9812
F	0.9630	0.9824	0.9827
Cl	0.9521	0.9776	0.9788
NO ₂	0.9334	0.9695	0.9733
substituent effect (CH ₃ – NO ₂)	0.0342	0.01415	0.0118
ρ^2 ^a	0.980	0.973	0.954

^a KIEs versus the Hammett σ constants.**TABLE 3: Experimental Chlorine Leaving Group KIEs for the S_N2 Reactions between Cyanide Ion and Four *Para*-Substituted Benzyl Chlorides at 20 °C in THF**

<i>para</i> -substituent	k^{35}/k^{37}			
	trial I	trial II	trial III	average
CH ₃	1.00609 \pm 0.00014 ^a			
H	1.00591 \pm 0.00004			
Cl	1.00546 \pm 0.00016	1.00527 \pm 0.00009 ^a	1.00540 \pm 0.00037 ^a	1.00537 \pm 0.00024 ^b
NO ₂	1.00556 \pm 0.00013	1.00568 \pm 0.00009		1.00562 \pm 0.00013 ^c

^a Standard deviation for 5 separate experiments measuring the KIE. ^b Standard deviation for 14 separate experiments measuring the KIE. ^c Standard deviation for 9 separate experiments measuring the KIE.**TABLE 4: Calculated C $_{\alpha}$ –Cl Bond Length in Five *Para*-Substituted Benzyl Chlorides at 25 °C Using Three Different Levels of Theory**

<i>para</i> -substituent	C $_{\alpha}$ –Cl bond length (Å)		
	RHF/6-31+G(d)	B3LYP/6-31+G(d)	B3LYP/aug-cc-pVDZ
CH ₃	1.8107	1.8442	1.8490
H	1.8086	1.8413	1.8451
F	1.8085	1.8400	1.8449
Cl	1.8063	1.8400	1.8455
NO ₂	1.8005	1.8314	1.8364
substituent effect (CH ₃ – NO ₂)	0.0102	0.0128	0.0126
ρ^2 ^a	0.997	0.970	0.926

^a C $_{\alpha}$ –Cl bond length versus the Hammett σ constants.**TABLE 5: Calculated C $_{\alpha}$ –Cl and NC–C $_{\alpha}$ Transition-State Bond Lengths for the S_N2 Reactions between Cyanide Ion and Five *Para*-Substituted Benzyl Chlorides at 25 °C Using Three Different Levels of Theory**

<i>para</i> -substituent	(C $_{\alpha}$ –Cl) ‡ bond length (Å)			(NC–C $_{\alpha}$) ‡ bond length (Å)		
	RHF/6-31+G(d)	B3LYP/6-31+G(d)	B3LYP/aug-cc-pVDZ	RHF/6-31+G(d)	B3LYP/6-31+G(d)	B3LYP/aug-cc-pVDZ
CH ₃	2.3592	2.2844	2.2705	2.3984	2.3941	2.3836
H	2.3466	2.2757	2.2619	2.3857	2.3884	2.3778
F	2.3474	2.2746	2.2621	2.3858	2.3857	2.3771
Cl	2.3292	2.2633	2.2505	2.3670	2.3786	2.3697
NO ₂	2.2872	2.2267	2.2145	2.3247	2.3508	2.3469
substituent effect (CH ₃ – NO ₂)	0.0720	0.0557	0.0560	0.0737	0.0433	0.0367
ρ^2 ^a	0.993	0.994	0.990	0.995	0.999	0.999

^a Transition-state bond lengths versus the Hammett σ constants.

trend; i.e., the KIE becomes smaller when a more electron-withdrawing substituent is present for the *para*-methyl- through the *para*-chloro- but then increases for the *para*-nitro- substituent. The KIEs for the *para*-chloro- and *para*-nitrobenzyl chlorides were remeasured to ensure that the KIE for the *para*-nitrobenzyl chloride was really greater than that found for the *para*-chlorobenzyl chloride. The results and the averages show that the KIEs for these two reactions are reproducible and that the KIE for the *para*-nitrobenzyl chloride is indeed greater than that for the *para*-chlorobenzyl chloride. This means there is no clean trend in these KIEs when a more electron-withdrawing substituent is on the benzene ring of the substrate.

The C $_{\alpha}$ –Cl ground-state and transition-state bond lengths and the k^{35}/k^{37} s for these reactions were calculated at several levels of theory, Tables 4–6, to demonstrate that the results were not restricted to a particular level of theory. Although there are differences in the C $_{\alpha}$ –Cl bond lengths in the ground state and transition state and in the KIEs predicted by the different levels of theory, the general trend is that the ground-state and transition-state C $_{\alpha}$ –Cl bond lengths and the chlorine KIEs in Tables 4–6 decrease when a more electron-withdrawing substituent is present. It is worth noting that the B3LYP/aug-cc-pVDZ calculations give the best agreement with the experimental KIEs. This is in agreement with the study by Fang

TABLE 6: Chlorine (k^{35}/k^{37}) Leaving Group KIEs for the S_N2 Reactions between Cyanide Ion and Five *Para*-Substituted Benzyl Chlorides at 25 °C Using Three Different Levels of Theory and Unscaled Frequencies

<i>para</i> -substituent	k^{35}/k^{37}		
	RHF/6-31+G(d)	B3LYP/6-31+G(d)	B3LYP/aug-cc-pVDZ
CH ₃	1.01012	1.00742	1.00717
H	1.01004	1.00743	1.00717
F	1.01003	1.00741	1.00716
Cl	1.00987	1.00728	1.00699
NO ₂	1.00950	1.00703	1.00676
substituent effect (CH ₃ – NO ₂)	0.00062	0.00039	0.00041
ρ^2 ^a	0.991	0.949	0.942

^a KIEs versus the Hammett σ constants.**TABLE 7: Experimental Chlorine (k^{35}/k^{37}) Leaving Group KIEs^{a,b} for the S_N2 Reactions of *Para*-Substituted Benzyl Chlorides with Various Nucleophiles at 20 °C**

<i>para</i> -substituent	k^{35}/k^{37}			
	C ₆ H ₅ S [−]	I [−]	C ₄ H ₉ S [−]	CH ₃ O [−]
CH ₃	1.00931	1.00996	1.00894	1.00780
H	1.00948		1.00920	1.00800
Cl	1.00990	1.00973	1.00915	1.00806
NO ₂	1.00918	1.00976	1.00871	1.00768
Average	1.00947	1.00982	1.00900	1.00789
Standard deviation	0.00031	0.00013	0.00022	1.00018

^a The error on each KIE was reported as 0.00010. ^b The data is taken from ref 33.

et al.²³ It is also worth noting that although scaling the frequencies in the calculations alters the magnitude of the chlorine KIEs it does not affect the trend (substituent effect) in the KIEs. Finally, adding solvent to the calculation using a solvent continuum model does not affect the trend in the chlorine KIEs either.

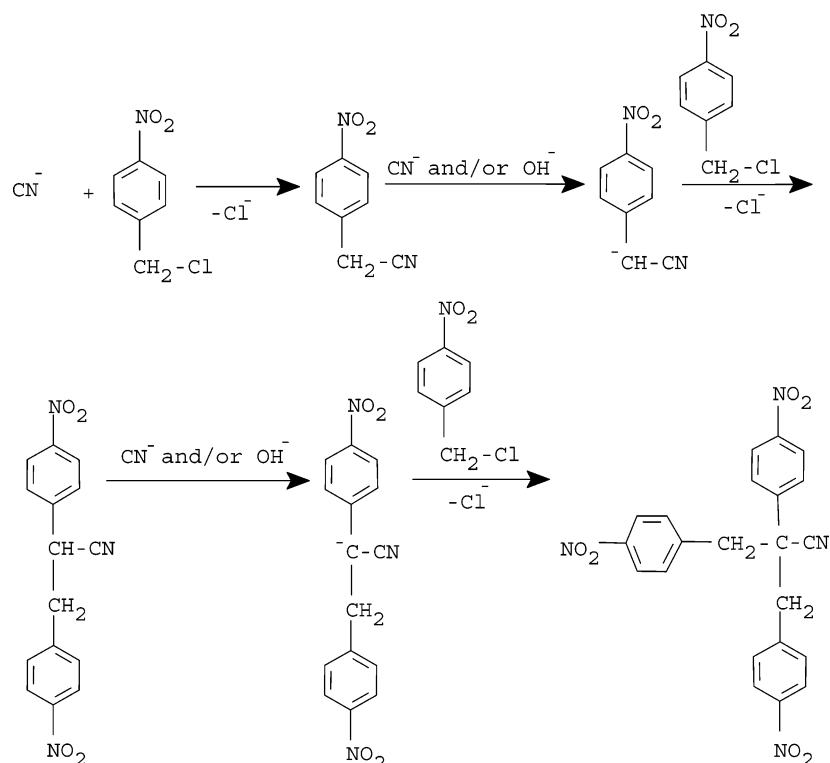
The substituent effect on the calculated parameters was again checked by plotting the calculated parameter in Tables 4–6 against the Hammett σ value for each substituent.³² All of the calculated parameters behaved as one would expect; i.e., the correlation coefficient for each plot was very high, ranging from 0.926 to 0.997 for the ground-state C_α–Cl bond lengths, from 0.990 to 0.994 for the transition-state C_α–Cl bond lengths, and from 0.942 to 0.991 for the chlorine KIEs. It is interesting that again the worst fit with the Hammett σ values is found with the calculations using the largest basis set and that the best fit is with the RHF/6-31+G(d) calculations. However, the correlation coefficients in all the Hammett σ plots are very high, giving one great confidence that the trends predicted by the calculations are correct.

The calculated KIEs, Table 6, decrease as a more electron-withdrawing substituent is added to the substrate whereas the experimental KIEs, Table 3, only decrease from the *para*-methylbenzyl chloride to the *para*-chlorobenzyl chloride and the KIE found for the *para*-nitrobenzyl chloride reaction is larger than the KIE for the *para*-chlorobenzyl chloride reaction. It is worth noting that this same inconsistency arose in Grimsrud's study³³ of the chlorine KIEs for a series of S_N2 reactions of *para*-substituted benzyl chlorides and several different nucleophiles, Table 7; i.e., the chlorine KIE for the *para*-nitrobenzyl chloride reaction was larger than the KIE for the *para*-chlorobenzyl chloride reaction when the nucleophile was iodide ion. Because (1) the chlorine leaving group KIE for the *para*-nitrobenzyl chloride reaction was smaller than the KIE for the *para*-chlorobenzyl chloride reaction when the nucleophile was thiophenoxide ion, *n*-butyl thiolate anion, or methoxide ion as expected and (2) the calculations indicate that the KIE for the

para-nitrobenzyl chloride reaction should be smaller than the KIE for the *para*-chlorobenzyl chloride reaction, the *para*-nitrobenzyl chloride reactions with cyanide ion and iodide ion were re-examined. High-performance liquid chromatography (HPLC) analyses showed that both reactions yielded several products. In particular, the *para*-nitrobenzyl chloride–cyanide ion reaction gave several products with the main product being a trimer possibly formed by the mechanism shown in Scheme 1.^{34,35} Also, since significant amounts of the trimer were found before all of the substrate was consumed, the chlorine is removed from the *para*-nitrobenzyl chloride in several different reactions, and the observed chlorine KIE is not due to the simple S_N2 reaction with the cyanide ion. Another indication that the reaction is not clean is that spin trap reagents and electron paramagnetic resonance spectroscopy³⁶ showed that the reactions between *para*-nitrobenzyl chloride and both iodide ion and cyanide ion contained radicals. Thus, neither of these reactions are the simple S_N2 reactions that had been supposed. This means the chlorine leaving group KIE for the *para*-nitrobenzyl chloride reaction should not be considered in determining if chlorine KIEs can be used to determine the relative amount of C_α–Cl bond rupture in the transition states of the cyanide ion–*para*-substituted benzyl chloride S_N2 reactions. In fact, it is important to note that the plot of the chlorine KIEs versus the Hammett σ values for the *para*-methyl- to the *para*-chloro- substituents in these *para*-substituted benzyl chloride–cyanide ion S_N2 reactions has a correlation coefficient of 0.982. Thus, both the calculated and the experimental chlorine KIEs indicate that one should be able to use the chlorine leaving group KIE to determine the substituent effect (the relative amount of C_α–Cl bond rupture) on the transition states of S_N2 reactions. Finally, it is worth noting that this trend in chlorine leaving group KIEs with substituent has been observed experimentally in several S_N2 reactions.^{2,8,12}

Nucleophile Carbon k^{11}/k^{14} KIEs. The nucleophile carbon k^{11}/k^{14} KIEs, Table 8, were measured to learn whether these KIEs could be used to determine the substituent effect on the NC–C_α transition-state bond for the cyanide ion–*para*-substituted benzyl chloride S_N2 reactions. An analysis of these nucleophile carbon KIEs and their errors suggests that there is no measurable trend in the KIE with a change in substituent.

All three levels of theory suggest that the NC–C_α transition-state bond becomes shorter, Table 5, and the nucleophile carbon KIE, Table 9, becomes more inverse (NC–C_α bond formation is more complete) in the transition state when a more electron-withdrawing substituent is on the benzene ring of the substrate. It is important to note that the changes in the NC–C_α transition-state bond and the KIEs predicted by all three levels of theory correlate extremely well with the Hammett σ values of the *para*-substituent. The correlation coefficients for the plots relating the length of the NC–C_α transition-state bond and the Hammett

SCHEME 1: Possible Mechanism for the Reaction Forming the Largest Side Product from the Reaction between Tetrabutylammonium Cyanide and *para*-Nitrobenzyl Chloride in THF at 20 °C

TABLE 8: Experimental Nucleophile Carbon k^{11}/k^{14} KIEs for the S_N2 Reactions between Cyanide Ion and Three *Para*-Substituted Benzyl Chlorides at 20 °C

<i>para</i> -substituent	k^{11}/k^{14}
CH ₃	$0.99951 \pm 0.0013^a (8)^b$
H	$1.00467 \pm 0.0009 (6)$
Cl	$1.00158 \pm 0.0025 (9)$

^a Standard deviation. ^b The number of separate evaluations of the KIE used to calculate the average KIE.

σ constant for the *para*-substituent are 0.997 for all three levels of theory, and the correlation coefficients for the KIE versus the Hammett σ values for the substituent range from 0.995 to 0.999. It is also important to note that the substituent effect on the length of the NC–C $_{\alpha}$ transition-state bond predicted by theory is consistent with the results of several experimental studies that have used KIEs and Hammett σ values to determine the substituent effect on the lengths of the Nu–C $_{\alpha}$ transition-state bonds in S_N2 reactions.^{5,8,10,12,31}

Although all three levels of theory suggest that the NC–C $_{\alpha}$ transition-state bond shortens when a more electron-withdrawing substituent is present, this change was not detected experimentally. However, two of the three theoretical methods, Table 5, showed that the change in the NC–C $_{\alpha}$ transition-state bond with substituent was smaller than the corresponding change in the C $_{\alpha}$ –Cl transition-state bond with substituent; i.e., the (change in the C $_{\alpha}$ –Cl/change in the NC–C $_{\alpha}$) transition-state bond with substituent is 1.53 for the B3LYP/aug-cc-pVDZ level of theory, 1.33 for the B3LYP/6-31+G(d) level of theory, and 1.00 for the RHF/6-31+G(d) level of theory. This much smaller change in the NC–C $_{\alpha}$ transition-state bond with substituent is probably why the change in the nucleophile carbon KIE was too small to detect experimentally.

Finally, it is interesting that the difference in the nucleophile KIEs with level of theory, Table 9, is much smaller than for the difference in the chlorine leaving group KIEs, Table 6, with

level of theory. For example, the difference in the nucleophile KIE with level of theory is $\leq 1\%$ whereas the difference in the chlorine leaving group KIE with level of theory is approximately 40%. Another observation is that the nucleophile KIE was not as close to the experimental value as the chlorine KIEs. The calculated chlorine KIEs at the B3LYP/aug-cc-pVDZ level differ from the experimental values by only approximately 0.0012 whereas the calculated nucleophile carbon KIEs differ from the experimental values by approximately 0.020. This difference between the theoretical and the experimental values is even clearer if one considers the percent difference between the experimental and theoretical values of the KIEs. The average percent difference in the chlorine KIEs is approximately $0.0012/0.0058 \times 100 = 21\%$ while that for the nucleophile carbon KIEs is approximately $0.0192/0.0019 \times 100 = 1011\%$. This same problem, i.e., that the difference between the calculated and experimental KIE was larger for the nucleophile carbon KIEs than for the leaving group KIEs, was observed in our previous study.²³

Substituent Effect on Transition-State Structure. Both the experimental and the theoretical substituent effect on the C $_{\alpha}$ –Cl transition-state bond, Tables 5 and 6, is that it becomes shorter when a more electron-withdrawing substituent is on the benzene ring. The calculated transition-state structures and nucleophile carbon KIEs, Tables 5 and 9, indicate that the NC–C $_{\alpha}$ transition-state bond also shortens, but by a smaller amount, when a more electron-withdrawing substituent is present. Thus, the calculations suggest that the transition state becomes tighter when a more electron-withdrawing substituent is present but that the greatest change in structure is in the C $_{\alpha}$ –Cl transition-state bond. It is worth noting that this result is predicted by Westaway's "Bond Strength Hypothesis",³⁷ which states that the greatest change in structure with substituent will be in the weaker reacting bond, i.e., in this case, the C $_{\alpha}$ –Cl bond. It is also important to note that the experimental

TABLE 9: Nucleophile Carbon k^{11}/k^{14} KIEs for the S_N2 Reactions between Cyanide Ion and Five *Para*-Substituted Benzyl Chlorides at 25 °C Using Three Different Levels of Theory

<i>para</i> -substituent	k^{11}/k^{14}		
	RHF/6-31+G(d)	B3LYP/6-31+G(d)	B3LYP/aug-cc-pVDZ
CH ₃	0.97604	0.98259	0.98381
H	0.97476	0.98202	0.98329
F	0.97470	0.98173	0.98311
Cl	0.97292	0.98105	0.98248
NO ₂	0.96874	0.97873	0.98079
substituent effect (CH ₃ – NO ₂)	0.00730	0.00386	0.00302
ρ^2 ^a	0.995	0.999	0.999

^a KIEs versus the Hammett σ constants.**TABLE 10: Individual Contributions to the Chlorine Leaving Group KIEs for the S_N2 Reactions between Cyanide Ion and Four *Para*-Substituted Benzyl Chlorides at 25 °C in the Gas Phase at the B3LYP/aug-cc-pVDZ Level of Theory**

<i>para</i> -substituent	TDF _R	KIE _T	TIF [‡]	TDF [‡]	KIE [‡] = {KIE _T × TIF [‡] × TDF [‡] }	total k^{35}/k^{37}
CH ₃	1.00714	1.00043	1.00215	0.99744	1.00002	1.00717
H	1.00725	1.00043	1.00210	0.99738	0.99991	1.00717
Cl	1.00725	1.00043	1.00201	0.99730	0.99973	1.00699
NO ₂	1.00758	1.00040	1.00174	0.99706	0.99919	1.00676
substituent effect (CH ₃ – NO ₂)	−0.00044	0.00003	0.00041	0.00038	0.00083	0.00041

KIEs, as far as is possible, confirm this trend in the transition-state structure with substituent. It is also important to note that these changes in transition-state structure with substituent have been found in other studies of the substituent effect on the transition-state structure of S_N2 reactions.^{2,5,8,10,12,31} The important conclusion of this study is that with some reservations (vide infra) both leaving group and nucleophile KIEs should be able to determine the substituent effects on transition-state structure as had been previously believed.

Implications of the Theoretical Study on Using Leaving Group Chlorine KIEs To Determine the Substituent Effect on the Transition States of S_N2 Reactions. The chlorine leaving group KIE can be expressed as

$$\text{KIE} = \text{TDF}_R \times \text{KIE}_T \times \text{TIF}^\ddagger \times \text{TDF}^\ddagger = \text{TDF}_R \times \text{KIE}^\ddagger \quad (4)$$

where the transition-state contribution to the total KIE, KIE[‡], is the product of the tunneling KIE, KIE_T, the imaginary frequency ratio for the reactions with the ³⁵Cl and ³⁷Cl isotopes, TIF[‡], and the isotope effect on the vibrational energy of the transition state, TDF[‡]. TDF_R represents the isotope effect on the vibrational energy of the reactants. TDF_R and TDF[‡] can be calculated²¹ from

$$\text{TDF}_R = \prod_i^{3N-6} [(\mu_i^R \sinh(\mu_i^R/2))/(\mu_i^R \sinh(\mu_i^R/2))] \quad (5)$$

and

$$\text{TDF}^\ddagger = \prod_i^{3N^\ddagger-7} [(\mu_i^\ddagger \sinh(\mu_i^\ddagger/2))/(\mu_i^\ddagger \sinh(\mu_i^\ddagger/2))] \quad (6)$$

respectively, where R represents the substrate, ‡ indicates the transition state, $\mu_i = h\nu_i/k_B T$, and the ν_i 's are the frequencies. KIE_T was calculated using the Wigner approximation.²⁵

Magnitude of the KIE versus the Percent C_α–Cl Bond Rupture in the Transition State. The individual contributions to the total chlorine leaving group KIEs, Table 10, shed light on the origin of these KIEs and have significant implications for those using these KIEs to determine the substituent effect on transition-state structure. The first important observation is

that the KIE[‡] contribution to the total KIE is very close to unity for all of the reactions; i.e., KIE[‡] ranges from 1.00002 to 0.99919. This means the KIE[‡] only accounts for approximately 10% of the total KIE and that the total KIE is mainly determined by TDF_R! The KIE[‡] contribution is smaller than the TDF_R contribution to the total KIE because the TDF[‡] contributions to the KIE are only 36–38% of the contributions due to TDF_R. This is reasonable because the vibrational energy of the C_α–Cl bond in the transition state is smaller than that in the substrate. In fact, TDF[‡] will make a smaller and smaller contribution (the TDF[‡] will approach 1.00000) to the total KIE as the amount of C_α–Cl bond rupture in the transition state increases. Both the KIE_T and the TIF[‡] also approach 1.00000 as the amount of C_α–Cl bond rupture in the transition state increases. This means that the KIE will increase with the amount of C_α–Cl bond rupture in the transition state for a particular reaction. This is undoubtedly why Paneth and co-workers¹⁹ found that the KIEs in their methyl chloride S_N2 reactions did not approach the expected maximum value of 1.019 but were bunched between 1.006 and 1.009 regardless of the amount of C_α–Cl bond rupture in the transition state. It is worth noting that the product {KIE_T × TIF[‡]} makes a significant contribution to the total KIE; i.e., the {KIE_T × TIF[‡]} represents between 34% and 38% of the total chlorine KIEs in Table 10. This is in agreement with the earlier study¹⁹ of 26 methyl chloride S_N2 reactions where the KIE_T and TIF[‡] terms represented a significant contribution to the total KIE. Finally, it is interesting that the KIE_T is less than 10% of the TIF[‡] contribution to the KIE.

Substituent Effects on the Chlorine Leaving Group KIEs.

A detailed examination of the substituent effect on each of the terms in the calculated chlorine leaving group KIEs, Table 10, shows that the substituent effect (KIE contribution for the *para*-methylbenzyl chloride reaction – KIE contribution for the *para*-nitrobenzyl chloride reaction) on the TDF_R and TDF[‡] terms are of almost identical magnitude; i.e., they are −0.00044 and +0.00038, respectively, even though the absolute magnitude of the TDF_R term is approximately 2.7 times greater than the TDF[‡] term. This is interesting because it suggests that changing a substituent changes the vibrational energy of the full C_α–Cl and partial (C_α...Cl) transition-state bond by the same relative amount.

TABLE 11: Substituent Effects on the Transition Structures and Chlorine Leaving Group KIEs for Different S_N2 Reactions with a Series of *Para*-Substituted Benzyl Chlorides at 25 °C Using the B3LYP/aug-cc-pVDZ Level of Theory

<i>para</i> -substituent	nucleophile									
	CN [−]		Cl [−]		Br [−]		<i>p</i> -O ₂ N-C ₆ H ₄ N		NH ₃	
	(% bond extension) [†]	<i>k</i> ³⁵ / <i>k</i> ³⁷	(% bond extension) [†]	<i>k</i> ³⁵ / <i>k</i> ³⁷	(% bond extension) [†]	<i>k</i> ³⁵ / <i>k</i> ³⁷	(% bond extension) [†]	<i>k</i> ³⁵ / <i>k</i> ³⁷	(% bond extension) [†]	<i>k</i> ³⁵ / <i>k</i> ³⁷
CH ₃	22.8	1.00717	32.2	1.00864	36.9	1.00884	42.5	1.00617	43.8	1.00650
H	22.6	1.00717	32.1	1.00858	36.6	1.00871	42.3	1.00625	43.5	1.00665
Cl	21.9	1.00699	31.4	1.00834	35.8	1.00860	41.8	1.00632	43.6	1.00666
NO ₂	20.6	1.00676	30.3	1.00792	34.3	1.00814	41.1	1.00620	42.6	1.00680
substituent effect (CH ₃ − NO ₂)	2.2	0.00041	1.9	0.00072	2.6	0.00070	1.4	0.00003	0.6	−0.00030

Another important observation is that the substituent effect on KIE[‡] is greater (+0.00083) than the substituent effect on the TDF_R contribution (−0.00044) to the KIE and that this greater change in the KIE[‡] contribution to the total KIE is responsible for the decrease in the total KIE with the electron-withdrawing ability of the substituent. This is important because the TDF_R term increases with the electron-withdrawing ability of the substituent, i.e., increases in the opposite direction. The surprising finding is that the substituent effect on the KIE[‡] term is only greater than the substituent effect on the TDF_R term because the substituent effect on the TDF[‡], the TIF[‡], and the KIE_T are all in the same direction; i.e., they each decrease with a more electron-withdrawing *para*-substituent. In fact, without the effect of the TIF[‡] and KIE_T, the change in the total KIE with substituent would be very small and in the opposite (wrong) direction since the calculations show that the C_α–Cl transition-state bond is shorter when a more electron-withdrawing substituent is present in every reaction.

An analysis of the data in Table 10 led to the important conclusion that the substituent effect on the KIE is dependent on transition-state structure. Three different substituent effects are possible. For instance, the contribution by TDF[‡] to the total KIE will be effectively zero (TDF[‡] = 1.00000 for all substituents) for a series of reactions with a very product-like transition state, so little or no substituent effect will be found on this term. Also, since the imaginary frequency decreases as the amount of C_α–Cl bond rupture in the transition state increases, both the TIF[‡] and the KIE_T, which depend on the imaginary frequency, will also decrease to 1.00000 for a very product-like transition state, and the KIE will be given by the TDF_R term alone. In these cases, the substituent effect on the KIE will be opposite that expected from the calculated transition-state structures for the reactions; i.e., the substituent effect on the KIE will be opposite that found for the benzyl chloride–cyanide ion reactions in this study. A second possibility is when the amount of C_α–Cl bond rupture in the transition state is small; i.e., the transition state is very reactant-like. In these cases, the TIF[‡] and the KIE_T will all be > 1.00000 and near a maximum for the reaction, the substituent effect will be given by the larger KIE[‡] contribution to the KIE, and the expected substituent effect on the reactions will be found; i.e., a smaller KIE will be found for the *para*-nitrobenzyl chloride than for the *para*-methyl benzyl chloride reaction. The third possibility will occur at some intermediate amount of C_α–Cl bond rupture in the transition state where the magnitudes of the KIE[‡] and the TDF_R contributions to the KIE are approximately equal, i.e., where the (TDF_R × TDF[‡]) equals 1.00000. In this case, no substituent effect will be found.

The proposal that variable substituent effects on the chlorine leaving group KIEs could be observed was tested by calculating the transition-state structures and chlorine KIEs for four other S_N2 reactions of *para*-substituted benzyl chlorides at the B3LYP/

aug-cc-pVDZ level of theory. The reactions, which had Cl[−], Br[−], 4-nitropyridine, and NH₃ as the nucleophiles, were chosen for this investigation because the percent extension of the C_α–Cl transition-state bond in the reaction with methyl chloride¹⁹ increased from 22% when the nucleophile was CN[−], to 31% when the nucleophile was Cl[−], to 34% when the nucleophile was Br[−], to 36.5% when the nucleophile was 4-nitropyridine, to 40% when the nucleophile was NH₃ and would represent a change from the reactant-like transition state for the CN[−] reaction to a product-like transition state for the NH₃ reaction; i.e., the product-like NH₃ transition state has N–C_α and C_α–Cl percent extensions, eq 3, of 15% and 42%, respectively. The results, Table 11, show that the normal (predicted by the transition-state structures for the reactions) substituent effect on the KIE is found when the nucleophile is CN[−], Cl[−] and Br[−], and the percent extension of the C_α–Cl transition-state bond is approximately 22%, 32%, and 36%, respectively, but that no substituent effect is found when the nucleophile is 4-nitropyridine and the percent extension of the C_α–Cl transition-state bond is approximately 42% and that the substituent effect is inverse when the nucleophile is NH₃ and the percent extension of the C_α–Cl transition-state bond is approximately 43%. It is important to note that these different substituent effects on the chlorine KIE are found even though the substituent effect on transition-state structure (the change in the percent extension of the C_α–Cl transition-state bond with substituent) is in the same direction for all five reactions; i.e., the C_α–Cl transition-state bond shortens when the *para*-substituent is more electron-withdrawing in all five reactions. This change in the substituent effect on the chlorine KIE as the amount of C_α–Cl bond rupture in the transition state increases is exactly what is predicted above. Finally, it is interesting that although the percent extension of the C_α–Cl transition-state bond in the *para*-substituted benzyl chloride series of reactions is slightly larger than those for the methyl chloride reactions they are not very different; i.e., the percent extension of the C_α–Cl transition-state bond in the (benzyl chloride/methyl chloride) reactions is 22.6/21.6 = 1.046, 32.1/30.6 = 1.049, 36.6/34.1 = 1.073, 42.3/36.5 = 1.16, and 43.5/39.6 = 1.098 for the CN[−], the Cl[−], the Br[−], the 4-nitropyridine and NH₃ nucleophiles, respectively. This is consistent with a slightly looser S_N2 transition state for the benzyl chloride series of reactions as is expected. It is also interesting that the increased looseness of the transition states for the benzyl chloride reaction relative to the methyl chloride reaction increases when poor nucleophiles are used in the reaction.

Substituent Effects on Nucleophile KIEs. An analysis of the data in Table 12 also suggests that different substituent effects will be found on the nucleophile KIE. First, the substituent effect (KIE contribution for the *para*-methylbenzyl chloride reaction − KIE contribution for the *para*-nitrobenzyl chloride reaction) on TDF[‡] is significantly larger than the

TABLE 12: Individual Contributions to the Calculated Nucleophile Carbon (k^{11}/k^{14}) KIEs for the S_N2 Reactions between Cyanide Ion and Five *Para*-Substituted Benzyl Chlorides at 25 °C in the Gas Phase at the B3LYP/aug-cc-pVDZ Level of Theory

<i>para</i> -substituent	TDF _R	KIE _T	TIF [‡]	TDF [‡]	KIE [‡] = {KIE _T × TIF [‡] × TDF [‡] }	total k^{11}/k^{14}
CH ₃	1.29637	1.00182	1.00905	0.75076	0.75893	0.98381
H	1.29637	1.00184	1.00898	0.75040	0.75853	0.98329
F	1.29637	1.00183	1.00886	0.75036	0.75839	0.98311
Cl	1.29637	1.00185	1.00876	0.74994	0.75791	0.98248
NO ₂	1.29637	1.00194	1.00854	0.74874	0.75660	0.98079
substituent effect (CH ₃ – NO ₂)	0.00000	–0.00012	0.00051	0.00202	0.00233	0.00302

TABLE 13: Substituent Effects on the Transition-State Structures and Nucleophile Carbon k^{11}/k^{14} and Nitrogen k^{14}/k^{15} KIEs for the S_N2 Reactions between Cyanide Ion and Ammonia with a Series of *Para*-Substituted Benzyl Chlorides, Respectively, at 25 °C Using the B3LYP/aug-cc-pVDZ Level of Theory

<i>para</i> -substituent	nucleophile			
	CN [–]		NH ₃	
	(% bond extension) [‡]	k^{11}/k^{14}	(% bond extension) [‡]	k^{14}/k^{15}
CH ₃	62.06	0.9838	15.67	0.9913
H	61.71	0.9833	15.58	0.9908
Cl	61.17	0.9831	14.74	0.9904
NO ₂	59.66	0.9808	14.21	0.9885
substituent effect (CH ₃ – NO ₂)	2.40	0.0030	1.46	0.0028

substituent effect on any other factor. For instance, it is 17 times larger than that on the TIF[‡] and even 5 times larger than that on the product {TIF × KIE_T}. Again, the substituent effect on the KIE_T is very small at approximately 20% of the substituent effect on the TIF[‡]. Of course, there is no substituent effect on the TDF_R because there is no bonding between the isotope and C_α in the ground state. Both the TDF_R and the TDF[‡] are large because of the strong C≡N bond in both the ground and the transition states. However, it is important to note that the inverse TDF[‡] is larger than the normal TDF_R. This is because the new C–C_α bond being formed in the transition state increases the vibrational energy of the carbon isotope in the C≡N[–].³⁸ This means the substituent effect on TDF[‡] is a major factor in determining the substituent effect on the nucleophile KIE.

Again, there will be a varying substituent effect on these KIEs. For a very reactant-like transition state with a long Nu–C_α bond, the (TDF_R × TDF[‡]) contribution to the total KIE will be for all intents and purposes 1.00000 because the bonding to the isotope in the reactant and the transition state will be virtually the same. The KIE_T and TIF[‡] will also be very close to 1.00000 for a very reactant-like transition state. Therefore, all of the KIEs will be equal to or very close to 1.00000, and no discernible substituent effect will be observed. If, however, the transition state is product-like with a short Nu–C_α bond, the TDF[‡] will be more inverse (larger) than the TDF_R, and since both the KIE_T and the TIF[‡] increase with the amount of bond formation in the transition state, the KIE will decrease with the amount of Nu–C_α bond formation in the transition state. Also, since the substituent effect on the product of the KIE_T and TIF[‡] is smaller than the substituent effect on TDF[‡], a measurable substituent effect on the KIE will be observed. The important discovery is that a larger and larger substituent effect on the nucleophile KIE will be found as the amount of Nu–C_α bond formation in the transition state increases.

The nitrogen (k^{14}/k^{15}) KIEs for the reactions between NH₃ and the *para*-substituted benzyl chlorides were calculated to test this suggestion. The carbon (k^{11}/k^{14}) and nitrogen (k^{14}/k^{15}) KIEs for the reactions with CN[–] and NH₃, respectively, Table 13, show that the substituent effect on the KIEs for these two reactions is effectively identical. However, considering that the maximum observed carbon KIE is approximately 5 times larger

than the maximum nitrogen KIE (1.22 versus 1.044),^{39,40} the substituent effect on the nitrogen KIEs represents a much greater change in the nitrogen KIEs than in the carbon KIEs (6.4% for the ¹⁴N/¹⁵N KIEs versus 1.3% for the ¹¹C/¹⁴C KIEs) as the above analysis suggests.

Conclusion

The important discovery from this study is that the substituent effect on both leaving group and nucleophile KIEs in S_N2 reactions vary with transition-state structure; i.e., one will only be able to observe a correct and measurable substituent effect on a C_α–LG bond using leaving group KIEs if C_α–LG bond rupture is significant but not well advanced in the transition state. Similarly, one will only be able to determine the substituent effect on the Nu–C_α transition-state bond using nucleophile KIEs when Nu–C_α bond formation is well advanced in the transition state, i.e., in a product-like S_N2 transition state. Thus, although the leaving group KIEs and nucleophile KIEs can, in principle, be used to determine substituent effects on transition-state structure, they will only be able to detect the correct substituent effect when the bond to the isotopic atom is short in the transition state. This is undoubtedly why different substituent effects on transition-state structure have been reported for S_N2 reactions. For example, in this study, the transition states have long NC–C_α (the average percent bond extension in these transition states is 61%) and relatively short C_α–Cl (the average bond extension in these transition states is 22%) bonds. Therefore, a measurable, expected, substituent effect for the chlorine leaving group KIEs and a very small or not measurable substituent effect on the nucleophile carbon KIEs is expected, and this is in fact what is observed both experimentally and computationally. Unlike this study where the nucleophile KIEs do not change significantly with substituent, the nucleophile k^{11}/k^{14} carbon KIEs decreased from 1.0119 to 1.0111 to 1.0096 when the *para*-substituent on the leaving group was changed from CH₃ to H to Cl (to a more electron-withdrawing group) in the S_N2 reactions between cyanide ion and in the S_N2 reactions between cyanide ion and *m*-chlorobenzyl-*para*-substituted benzenesulfonates, which were thought

to react via product-like transition states with short NC–C $_{\alpha}$ bonds.¹⁰ Paneth and co-workers⁹ also found a measurable substituent effect on the nucleophile nitrogen KIEs when a more electron-withdrawing substituent was on the benzene ring of the nucleophile in the S_N2 reactions between *para*-substituted *N,N*-dimethylanilines and methyl iodide. This clearly suggests that these reactions proceed via product-like transition states.

Different substituent effects on chlorine leaving group KIEs have also been observed in the S_N2 reactions of *para*-substituted benzyl chlorides. For instance, the chlorine leaving group KIEs for the S_N2 reactions between thiophenoxide ion, iodide ion, *n*-butyl thiolate ion and methoxide ion and *para*-substituted benzyl chlorides, Table 7, show no consistent trend in the chlorine KIEs with the electron-withdrawing ability of the substituent.^{5,13} In fact, the KIEs for 6 of the 11 possible comparisons increase, not decrease, when a more electron-withdrawing substituent is on the benzene ring of the substrate. However, in the S_N2 reactions between *para*-substituted benzyl chlorides and borohydride ion,^{12,13} the chlorine leaving group KIEs decrease significantly from 1.0076 to 1.0036 as the electron-withdrawing ability of the substituent increases. It has been suggested that the reactions in Table 7 have product-like transition states while the borohydride reactions have reactant-like transition states.

Finally, while this investigation of the leaving group and nucleophile KIEs suggests the usefulness of these KIEs for determining the substituent effects on transition-state structure is limited, all is not lost. The failure to see a measurable substituent effect on a leaving group or nucleophile KIE indicates that the bond to the isotope is long in the transition state of the S_N2 reaction. Thus, as well as being able to determine the substituent effect on transition-state structure in some S_N2 reactions, these KIEs can indicate whether an S_N2 reaction has a reactant-like, a product-like, or a central transition state.

Experimental Section

Secondary α -Deuterium KIEs. Approximately 0.9 g of tetrabutylammonium cyanide was dissolved in 50 mL of anhydrous THF under a nitrogen atmosphere in an I²R (Instruments for Research and Industry, Inc.) glove bag. Then, a 0.060–0.70 M stock solution of benzyl chloride was prepared in a sample vial that had been prefilled with 10 mL of anhydrous THF and sealed with a rubber septum under a nitrogen atmosphere in the glove bag by injecting 1 mL of benzyl chloride into the sample vial. The exact concentration of the benzyl chloride stock solution was calculated from the accurate weight of the vial before and after the benzyl chloride was added. Then, 20 mL of the tetrabutylammonium cyanide stock solution was transferred into a reaction flask fitted with a serum cap in the glove bag, and the reaction flask and the benzyl chloride stock solution were cooled in a distilled ice–water bath for an hour. The reaction was started by injecting 1.00 mL of the benzyl chloride stock solution into the reaction flask. One milliliter samples of the reaction mixture solution were taken at various times throughout the reaction and injected into 25 mL of 0.0025 M nitric acid to quench the reaction by converting the unreacted cyanide ion into HCN. The acidic solution was stirred in the fume hood for at least an hour to completely remove the HCN and then the chloride ion in the sample was analyzed in a potentiometric titration using a standard 0.005 M silver nitrate solution.

The same procedure was used to measure the secondary α -deuterium KIE except that the tetrabutylammonium cyanide

stock solution was prepared by dissolving 0.5 g of tetrabutylammonium cyanide in 50 mL of anhydrous THF and that the 4-chlorobenzyl chloride solution was prepared by injecting 0.58 mL of 4-chlorobenzyl chloride in a sample vial containing 10 mL of anhydrous THF.

Chlorine Leaving Group KIEs. The procedure used in measuring these KIEs is described in ref 17.

Nucleophile Carbon k^{11}/k^{14} KIEs. *Reagents.* The aldehyde impurities in the *para*-substituted benzyl chlorides were removed by treatment with sodium bisulfite.^{41,42} Then, the purified compounds were distilled under reduced pressure and stored in an airtight container in the refrigerator. ¹H NMR showed negligible levels of aldehyde after a week. The THF was distilled over sodium and benzophenone. The tetrabutylammonium cyanide (TBACN) was stored in a desiccator over P₂O₅. To avoid a buildup of [¹⁴C]formic acid, small aliquots of the solid [¹⁴C]potassium cyanide (2.04 GBq/mmol, American Radiolabeled Chemicals, Inc.) were withdrawn and dissolved in distilled water on the day of a kinetic run. Any unused K[¹⁴C]N solution was refrigerated and used within 2 days. The ¹¹C-labeled cyanide was produced employing the Scanditronix MC-17 Cyclotron at Uppsala Imanet AB. Proton bombardment of nitrogen, ¹⁴N-(p, α)¹¹C, in the presence of trace amounts of oxygen afforded [¹¹C]O₂, which was converted to hydrogen [¹¹C]cyanide utilizing an on-line gas-processing synthesis.^{43,44} Prior to trapping in distilled water (1 mL at 0 °C) the H[¹¹C]N was passed through a 50% aqueous sulfuric acid at 70 °C and then Sicapent. All of the work with ¹¹C materials was performed behind 5-cm-thick lead shields. Generally, the resulting activity of the H[¹¹C]N solution was 2.0–4.0 GBq.

After transport to the laboratory in a lead-lined trolley, sufficient [¹⁴C]potassium cyanide to yield a ¹⁴C activity of over 10 000 counts per min at 50% reaction of a kinetic run, was added to the [¹¹C]hydrogen cyanide solution. Impurities mostly formed in the synthesis of H[¹¹C]N were removed by employing a preparative HPLC system equipped with a β^+ -detector and a C18 column (Phenomenex, Luna 10 μ m, 250 mm \times 10 mm) operating at a flow of 4 mL/min. The isocratic mobile-phase system consisted of ammonium formate (50 mM, pH 3.5) 95% and acetonitrile 5%. Hydrochloric acid (0.3 mL, 0.11 mM) was added to the collected fraction of HCN (t_R = 4.5–5.1 min). Then, the HCN was transferred to the reaction solvent by heating the solution to 75 °C and passing a gentle stream of nitrogen (<10 mL/min) through the solution. The HCN was dried with Sicapent before being trapped in an anhydrous THF solution of TBACN (1.0 mL, 0.05 M) at –42 °C. The activity of the THF solution was usually 150–300 MBq after 7 min of distillation.

Kinetic Procedure. Two portions (100 and 700 μ L) of the labeled THF solution were withdrawn and transferred to septum-capped 1.5 mL vials. A 10 μ L aliquot was taken from the 700 μ L portion and mixed with 90 μ L of 30% acetonitrile in water. Dilution with water was necessary to prevent substantial tailing of the HCN peak, and the acetonitrile was needed to ensure full solubility of the *para*-substituted benzyl cyanides. Ten microliters of the diluted cyanide solution was injected into an HPLC equipped with a β^+ -flow detector. The HPLC consisted of a C18 column (Phenomenex, Synergy 4 μ m Hydro-RP 80 Å, 150 mm \times 4.60 mm) operating at a flow rate of 1 mL/min. The mobile-phase system consisted of ammonium formate, 50 mM at pH 3.5, (A) and acetonitrile (B). The gradient system used was: from 0 to 2 min, 7% B; from 2 to 3 min, 7 to 80% B; 3–8 min, 80% B; 8–9 min, 80 to 7% B; 9–16 min, 7% B. The product fraction (X = H, 6.8–8.5 min; CH₃, 6.3–8.0 min;

Cl, 6.6–8.3 min) was collected to serve as a correction for ¹⁴C impurities (see below). To achieve flexible and clean collection, a manual procedure was employed. The outlet from the β⁺-detector was elongated by Teflon tubing so that it could be directly immersed into a polyethylene scintillation vial containing 14 mL of Zinsser Analytic QUICKSAFE A scintillation cocktail. Immediately after collection, the outlet tube from the detector was withdrawn, and the vial was capped and shaken vigorously.

Sufficient *para*-substituted benzyl chloride (X = H, 6 μL; CH₃, 6.5 μL; Cl, 6 μL) to react with between 25% and 60% of the hydrogen cyanide was added to the capped vial containing the 700 μL of solution. After vortex mixing, the vial was placed in an autoinjector rack connected to a temperature bath at 20 ± 0.01 °C. Every 20 min, a 10–20 μL aliquot of the diluted reaction mixture was injected into the HPLC, and the product fraction was collected as described above. Care was taken to reseal the reaction vial with Parafilm after each injection. Twenty microliters of the neat *para*-substituted benzyl chloride was added to the 100 μL solution at the beginning of the experiment. This amount ensured complete reaction of the cyanide. At the end of the experiment, a 10 μL aliquot of this solution was withdrawn and diluted with 90 μL of acetonitrile (no water was added as to ensure full solubility of the *para*-substituted benzyl nitriles). 20 μL of the resulting solution was injected into the HPLC, and the product fraction collected as described above.

The total amount of radioactivity (¹¹C + ¹⁴C) in the collected fractions was measured by liquid scintillation at a wide mode for 2.5 min. Usually, the activity was 20 000–300 000 cpm (counts per min). When all of the ¹¹C had decayed, each sample was remeasured to obtain the ¹⁴C activity (wide mode, 50 min), which normally was 10 000–50 000 cpm. The time for each measurement was adjusted so that the relative error of the activity was less than 1%. To correct for possible ¹⁴C contaminants coeluting with the *para*-substituted benzyl cyanides, the initial labeled cyanide solution was injected twice, and fractions were taken at the *t_R* of the *para*-substituted benzyl cyanide. The mean of these activities and the activity of the product fraction from the unreacted cyanide solution was subtracted from the ¹⁴C activity. The ¹¹C activity was obtained by subtracting the uncorrected ¹⁴C activity from the (¹¹C + ¹⁴C) value. Finally, the ¹¹C activity was decay-corrected.

Data Evaluation. The kinetic isotope effect was calculated with eq 7

$$k^{11}/k^{14} = \ln(1 - f)/\ln[1 - f(R_f/R_0)] \quad (7)$$

The isotopic ratio *R_f* was calculated by dividing the corrected ¹⁴C and ¹¹C values at fraction of reaction, *f*, and *R₀* was the ratio of the corrected ¹⁴C and ¹¹C values at 100% reaction. The *f* value was obtained from the peak areas in the β⁺-detector chromatograms. A ¹¹C impurity coeluted with the hydrogen cyanide. The amount of impurity was obtained from the chromatogram of the 100% reaction sample and subtracted from the area of the reactant peak in each reaction chromatogram. Usually, the impurity represented 2.0–2.5% of the total activity. Since the impurity did not react and was constant throughout the experiment, the impurity, although unidentified, did not affect the results.

Acknowledgment. The authors gratefully acknowledge the support of the Natural Sciences and Engineering Research Council of Canada, the Swedish Science Research Council, and the Atlantic Computational Excellence Network for computer

time. A Carl Storm International Diversity Fellowship to S.M.I. to attend an Isotopes in the Biological and Chemical Sciences Gordon Research Conference is also gratefully acknowledged.

References and Notes

- Hudson, R. F.; Klopman, G. *J. Chem. Soc.* **1962**, 1062.
- Hill, J. W.; Fry, A. *J. Am. Chem. Soc.* **1962**, *84*, 2763.
- Ballistreri, F. P.; Maccarone, E.; Mamo, A. *J. Org. Chem.* **1976**, *41*, 3364.
- Westaway, K. C.; Ali, S. F. *Can. J. Chem.* **1979**, *57*, 1354–1367.
- Westaway, K. C.; Waszczylo, Z. *Can. J. Chem.* **1982**, *60*, 2500–2520.
- Ando, T.; Tanabe, H.; Yamataka, H. *J. Am. Chem. Soc.* **1984**, *106*, 2084.
- Lee, I.; Koh, H. J.; Lee, B.-S.; Sohn, D. S.; Lere, B. C. *J. Chem. Soc., Perkin Trans.* **1991**, *2*, 174.
- Matsson, O.; Persson, J.; Axelsson, B. S.; Langstrom, B.; Fang, Y.; Westaway, K. C. *J. Am. Chem. Soc.* **1996**, *118*, 6350–6354.
- Szylhabel-Godala, A.; Madhavan, S.; Rudzinski, J.; O'Leary, M. H.; Paneth, P. *J. Phys. Org. Chem.* **1996**, *9*, 35–40.
- Westaway, K. C.; Fang, Y.-r.; Persson, J.; Matsson, O. *J. Am. Chem. Soc.* **1998**, *120*, 3340–3344.
- Westaway, K. C.; Jiang, W. *Can. J. Chem.* **1999**, *77*, 879–889.
- Koerner, T.; Fang, Y.-r.; Westaway, K. C. *J. Am. Chem. Soc.* **2000**, *122*, 7342–7350.
- Westaway, K. C. *Adv. Phys. Org. Chem.* **2006**, *41*, 257–259.
- Kato, S.; Davico, G. E.; Lee, H. S.; DePuy, C. H.; Bierbaum, V. M. *Int. J. Mass Spectrom.* **2001**, *210/211*, 223.
- Hargreaves, R. T.; Katz, A. M.; Saunders, W. H., Jr. *J. Am. Chem. Soc.* **1976**, *98*, 2614–2617.
- Lynn, K. R.; Yankwich, P. E. *J. Am. Chem. Soc.* **1961**, *83*, 3220.
- Koerner, T.; Fang, Y.-r.; Westaway, K. C. *J. Am. Chem. Soc.* **2000**, *122*, 7342–7350.
- Shiner, V. J.; Wilgis, F. P. In *Heavy Atom Isotope Effects*; Buncl, E., Saunders, W. H., Jr., Eds.; Isotopes in Organic Chemistry 8; Elsevier: New York, 1992; pp 239–335.
- Dybala-Defratyka, A.; Rostkowski, M.; Matsson, O.; Westaway, K. C.; Paneth, P. *J. Org. Chem.* **2004**, *69*, 4900–4905.
- Melander, L. *Isotope Effects on Reaction Rates*; Ronald Press: New York, 1960; pp 15 and 34.
- Paneth, P. *Comput. Chem.* **1995**, *19*, 231–240.
- Fang, Y.; S. MacMillar, S.; Eriksson, J.; Kolodziejska-Huben, M.; Dybala-Defratyka, A.; Paneth, P.; Matsson, O.; Westaway, K. C. *J. Org. Chem.* **2006**, *71*, 4742–4747.
- Fang, Y.; Gao, Y.; Ryberg, P.; Eriksson, J.; Kolodziejska-Huben, M.; Dybala-Defratyka, A.; Madhavan, S.; Danielsson, R.; Paneth, P.; Matsson, O.; Westaway, K. C. *Chem. Eur. J.* **2003**, *9*, 2696–2709.
- Frisch, M. J.; Trucks, G. W.; Schlegel, H. B.; Scuseria, G. E.; Robb, M. A.; Cheeseman, J. R.; Montgomery, J. A., Jr.; Vreven, T.; Kudin, K. N.; Burant, J. C.; Millam, J. M.; Iyengar, S. S.; Tomasi, J.; Barone, V.; Mennucci, B.; Cossi, M.; Scalmani, G.; Rega, N.; Petersson, G. A.; Nakatsuji, H.; Hada, M.; Ehara, M.; Toyota, K.; Fukuda, R.; Hasegawa, J.; Ishida, M.; Nakajima, T.; Honda, Y.; Kitao, O.; Nakai, H.; Klene, M.; Li, X.; Knox, J. E.; Hratchian, H. P.; Cross, J. B.; Bakken, V.; Adamo, C.; Jaramillo, J.; Gomperts, R.; Stratmann, R. E.; Yazyev, O.; Austin, A. J.; Cammi, R.; Pomelli, C.; Ochterski, J. W.; Ayala, P. Y.; Morokuma, K.; Voth, G. A.; Salvador, P.; Dannenberg, J. J.; Zakrzewski, V. G.; Dapprich, S.; Daniels, A. D.; Strain, M. C.; Farkas, O.; Malick, D. K.; Rabuck, A. D.; Raghavachari, K.; Foresman, J. B.; Ortiz, J. V.; Cui, Q.; Baboul, A. G.; Clifford, S.; Cioslowski, J.; Stefanov, B. B.; Liu, G.; Liashenko, A.; Piskorz, P.; Komaromi, I.; Martin, R. L.; Fox, D. J.; Keith, T.; Al-Laham, M. A.; Peng, C. Y.; Nanayakkara, A.; Challacombe, M.; Gill, P. M. W.; Johnson, B.; Chen, W.; Wong, M. W.; Gonzalez, C.; Pople, J. A. *Gaussian 03*, revision B.05; Gaussian, Inc.: Wallingford, CT, 2004.
- Wigner, E. *Z. Phys. Chem. B* **1932**, *19*, 203.
- Anisimov, V.; Paneth, P. *J. Math. Chem.* **1999**, *26*, 75.
- (a) A. J. Gordon, R. A. Ford in *The Chemist's Companion: A Handbook of Practical Data, Techniques and References*; Wiley: New York, 1973; pp 6–7.
- Westaway, K. C.; Pham, T. V.; Fang, Y.-r. *J. Am. Chem. Soc.* **1997**, *119*, 3670–3676.
- Koshy, K. M.; Robertson, R. E. *J. Am. Chem. Soc.* **1974**, *96*, 914.
- Shiner, V. J., Jr.; Dowd, W.; Fisher, R. D.; Hartshorn, S. R.; Kessik, M. A.; Milakofsky, L.; Rapp, M. W. *J. Am. Chem. Soc.* **1969**, *91*, 4838.
- Westaway, K. C. In *Secondary Hydrogen–Deuterium Isotope Effects*; Buncl, E.; Lee, C. C., Eds.; Isotopes in Organic Chemistry 7; Elsevier: New York, 1987; pp 336–342.
- Gilliom, R. D. *Introduction to Physical Organic Chemistry*; Addison-Wesley: Reading, MA, 1970; pp 146–147.
- Grimsrud, E., Ph.D. Dissertation, University of Wisconsin, Madison, WI, 1971.

- (34) The tetrabutylammonium cyanide used in this study was only 95% pure. When tetrabutylammonium cyanide was dissolved in water, the solution had a pH greater than 11, suggesting that the contaminant was tetrabutylammonium hydroxide. However, it is not known whether the base in Scheme 1 is cyanide ion and/or hydroxide ion.
- (35) Both the trimer and the dimer proceeding it in Scheme 1 have been isolated from the reaction and identified by NMR spectroscopy.
- (36) Crozet, M. P.; Flesia, E.; Surzur, J. M.; Boyer, M.; Tordo, P. *Tetrahedron Lett.* **1975**, 4563.
- (37) Westaway, K. C. *Can. J. Chem.* **1993**, 71, 2084–2094.
- (38) Jobe, D. J.; Westaway, K. C. *Can. J. Chem.* **1993**, 71, 1353–1361.
- (39) Persson, J.; Berg, U.; Matsson, O. *J. Org. Chem.* **1995**, 60, 5037–1540.
- (40) Buddenbaum, W. E.; Shiner, V. J., Jr. In *Isotope Effects on Enzyme-Catalyzed Reactions*; Cleland, W. W., O'Leary, M. H., Northrop, D. B., Eds.; University Park Press: Baltimore, MD, 1977; p 18.
- (41) Shiner, R. L.; Fuson, R. C.; Curtin, D. Y. *The Systematic Identification of Organic Compounds*, 4th ed.; Wiley: New York, 1956; p 149.
- (42) Perrin, D. D.; Armarego, W. L. F. In *Purifications of Laboratory Chemicals*, 3rd ed.; Pergamon Press: Oxford, U. K., 1988; pp 60–61 and 367.
- (43) Iwata, R.; Ido, T.; Takahashi, T.; Nakanishi, H.; Iida, S. *Appl. Radiat. Isot.* **1987**, 38, 97–102.
- (44) Christman, D. R.; Finn, R. D.; Karlstrom, K. I.; Wolf, A. P. *Int. J. Appl. Radiat. Isot.* **1975**, 26, 435–442.